Available online at www.sciencedirect.com
ScienceDirect
International Journal of Heat and Mass Transfer 51 (2008) 4544–4550
International Journal of HEAT and MASS TRANSFER
www.elsevier.com/locate/ijhmt

Steam condensing – liquid CO_2 boiling heat transfer in a steam condenser for a new heat recovery system

Konstantin Nikitin, Yasuyoshi Kato *, Takao Ishizuka

Research Laboratory for Nuclear Reactors, Tokyo Institute of Technology, N1-2, 2-12-1 O-okayama, Meguro-ku, Tokyo 152-8550, Japan

Received 14 November 2006; received in revised form 5 December 2007
Available online 21 April 2008

Abstract

In a new waste heat recovery system, waste heat is recovered from steam condensers through cooling by liquid CO_2 instead of seawater, taking advantage of effective boiling heat transfer performance; the heat is subsequently used for local heat supply. The steam condensing – liquid CO_2 boiling heat transfer performance in a steam condenser with a shell and a helical coil non-fin tube was studied both numerically and experimentally. A heat transfer numerical model was constructed from two models developed for steam condensation and for liquid CO_2 boiling. Experiments were performed to verify the model at a steam pressure range of 3.2–5 kPa and a CO_2 saturation pressure range of 5–6 MPa. Overall heat transfer coefficients obtained from the numerical model agree with the experimental data within ±5%. The numerical estimations show that the boiling local heat transfer coefficient reaches a maximum value of 26 kW/m^2 K. This value is almost one order higher than that of a conventional water-cooled condenser.

Keywords: Steam condenser; Liquid CO_2; Boiling heat transfer; Heat recovery system; Waste heat

1. Introduction

In typical steam turbine cycles, steam of about 33 °C exhausted from turbines is condensed to water of the same temperature by taking seawater of about 20 °C into condensers. More than 40% of the energy generated from burning of fossil fuels, even in the most advanced gas-steam turbine combined power plants, is thereby dissipated into the environment through steam condensers.

In this new waste-heat recovery system, liquid CO_2 of 22 °C is used as a cooling medium in the condenser instead of seawater, as shown in Fig. 1. Heat transfer in the condenser of the waste heat recovery system is performed by steam condensation and liquid CO_2 boiling. The CO_2 gas generated through boiling of liquid CO_2 in the condenser is pressurized to 12 MPa using a compressor in a mechanical heat pump system; its temperature is raised to about 90 °C. The resultant CO_2 of 90 °C is used for heating water from 25 to 83 °C in the heat exchanger of the hot water supply system; its temperature is thereby lowered to 30 °C at 12 MPa. Hot water of 83 °C is delivered to office buildings, factories, swimming pools, and so on for local heat supply. The CO_2 of 30 °C is further cooled to 22 °C by reducing pressure from 12 to 5.9 MPa in an expander turbine. The liquid CO_2 of 22 °C and 5.9 MPa is used again for cooling steam in the condenser. No waste heat is released from the system to the environment because the condenser cooling loop is a closed circuit. The cogeneration system produces no waste heat pollution. The energy utilization factor of a combined power system is greater than 90% [1].

The local steam condensing heat transfer coefficient can be estimated using the modified Nusselt correlation developed by Kern [2]. This correlation has been widely used for designing industrial condensers. In the past, several attempts have been made to develop a model of heat transfer for CO_2 boiling. However, its boiling heat transfer model has not been well established. Hwang et al. [3] modified the Bennett and Chen [4] correlation for vertical tubes,

* Corresponding author. Tel.: +81 3 5734 3065; fax: +81 3 5734 2959.
E-mail address: kato.y.ad@m.titech.ac.jp (Y. Kato).

0017-9310/$ - see front matter © 2008 Elsevier Ltd. All rights reserved.
doi:10.1016/j.ijheatmasstransfer.2008.02.028

Nomenclature

A	heat transfer area, m^2
D	tube diameter, m
G	mass velocity, kg/m^2 s
g	gravitational acceleration, 9.81 m/s^2
h_{fg}	modified latent heat of vaporization, J/kg
HTC	heat transfer coefficient
i	enthalpy, J/kg
L	tube length, m
M	molecular weight
N	number of coils
P	pressure, Pa
Pr	Prandtl number
p_r	reduced pressure
Q	heat load, W
q	heat flux, W/m^2
R	tube radius, m
Re	Reynolds number
U	overall heat transfer coefficient, W/m^2 K
W	flow rate, kg/s
x	vapor quality
δ	thickness of annular liquid film, m
ε	cross-sectional vapor void fraction
θ	angle, rad
λ	thermal conductivity, W/m K
μ	dynamic viscosity, kg/m s
ρ	density, kg/m^3

Subscripts/superscripts

cb	convective boiling
CO_2	carbon dioxide side
dry	dry
H_2O	steam/water side
in	inner
L	liquid
nb	nucleate boiling
out	outer
sat	at saturated condition
tp	two-phase
V	vapor
wall	wall
wet	wet

applying six new empirical factors based on data of Bredesen et al. [5] for a horizontal tube with 7 mm inner diameter at one saturation temperature. Knudsen and Jensen [6] included some multipliers to the Shah [7] correlation to fit it to their data. Thome and Ribatski tested the empirical correlation models proposed by Yoon et al. [8], Hwang et al. [3], Thome and El Hajal [9], and Liu and Winterton [10] to reproduce the wide range of experimental data obtained by Bredesen et al. [5], Knudsen and Jensen [6], Yun et al. [11], Yoon et al. [8], and Koyama et al. [12] for macrochannel heat transfer. They concluded that the correlation model proposed by Thome and El Hajal among the four correlation models gave the best fit for the wide range of data [13].

In this study, the Thome and El Hajal model has been combined with the modified Nusselt correlation to develop a numerical model of steam condensing – liquid CO_2 boiling heat transfer for the steam condenser in the new waste heat recovery system. Its applicability was confirmed through comparison of numerical results with experimental data obtained from the mockup test facility for the heat recovery system.

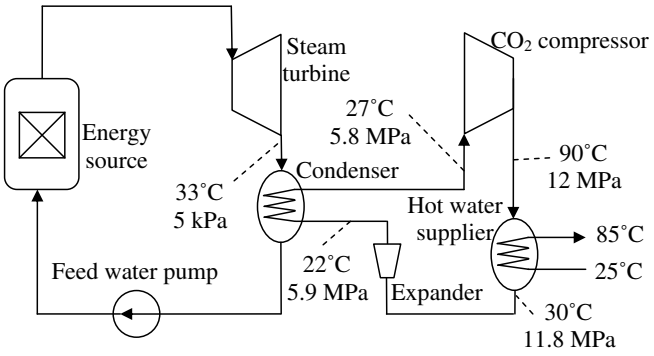

Fig. 1. Waste heat recovery system.

2. Test facility and experimental conditions

The experimental test facility shown in Fig. 2 comprises a steam generator with superheating, a condenser with a shell and a helical coil heat exchanger tube, a hot water supplier with a double tube heat exchanger, an expansion valve, etc. Both the heat exchanger tube of the condenser and the hot water supplier are made by copper. The con-

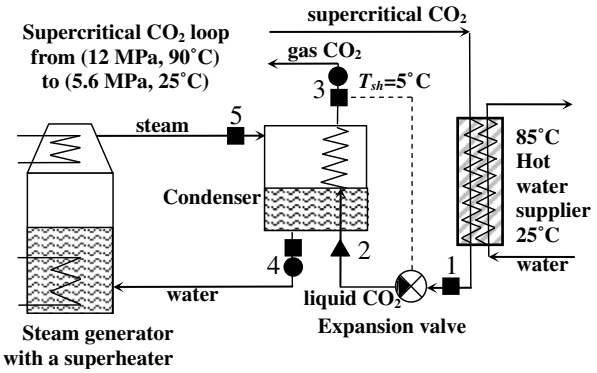

Fig. 2. Schematic diagram of test facility. T_{sh} is the CO_2 superheated temperature. Measurement: (■) temperature and pressure; (▲) pressure; (●) flow rate.

densed water is transferred back to the steam generator through natural circulation. The main measurement parameters are: the water temperature and flow rate at the inlet and outlet of the hot water supplier; CO_2 pressure, temperature and flow rate at the outlet of the condenser; steam temperature and pressure at the inlet of the condenser; and the condensed water temperature and flow rate at the outlet of the condenser. All of these parameters were recorded automatically with sampling frequency of 0.5 Hz.

Steam, water, and CO_2 pressure at the inlet and outlet of the condenser were measured using pressure gauge transducers with an accuracy of ±0.5% over the full range. The steam, water and CO_2 temperature were measured using T-type (copper/constantan) thermocouples with ±0.5 °C accuracy. The condensed water flow rate was measured using an electromagnetic flow meter with ±0.62% accuracy; whereas the gaseous CO_2 flow rate was measured using a Coriolis type flow meter with ±0.52% accuracy. The positions of the measurement equipment are shown in Fig. 2.

The CO_2 inlet pressure at the hot-water supplier was maintained at approximately 12 MPa; the expansion valve pressure was varied from 5 to 6 MPa. The CO_2 flow rate was controlled using the expansion valve with a Proportional, Integral, Derivative (PID) control system so that CO_2 superheating at the condenser outlet was maintained at 5 °C. The steam pressure was varied from 3.2 to 5 kPa. The steam superheat was set at 10 °C. The nominal heat load of 3 kW corresponds to the condensed water flow rate of 4.44 kg/h. The heat load increases with the condenser steam pressure because of the higher steam saturation temperature. The heat load also increases with decreasing CO_2 quality because of the enhancement of nucleate boiling heat transfer. The range of experimental conditions for the condenser is given in Table 1.

The shell and helical coil tube type condenser is shown in Fig. 3. The tube's inner and outer diameters are 7.13 and 9.53 mm. The tube wall thickness is 1.2 mm. The active tube length is 8.5 m. The condenser was placed into the shell of a 10-l vacuum vessel. The condenser tube of about 160 mm from the outlet is located under the condensed water level at the bottom of vessel. The heat transfer in this region is neglected both in experimental data treatment and in numerical simulation.

Table 1
Range of experimental conditions for the condenser

Parameters	Fluid	
	CO_2	H_2O
Type	Shell and helical coil tube	
	Helical coil tube	Shell
Maximal heat duty, kW	4.5	
Maximal flow rate, kg/h	100	6.6
Temperature range, °C	14–22	24–33
Pressure range, kPa	(5–6) × 10^3	3.2–5.0

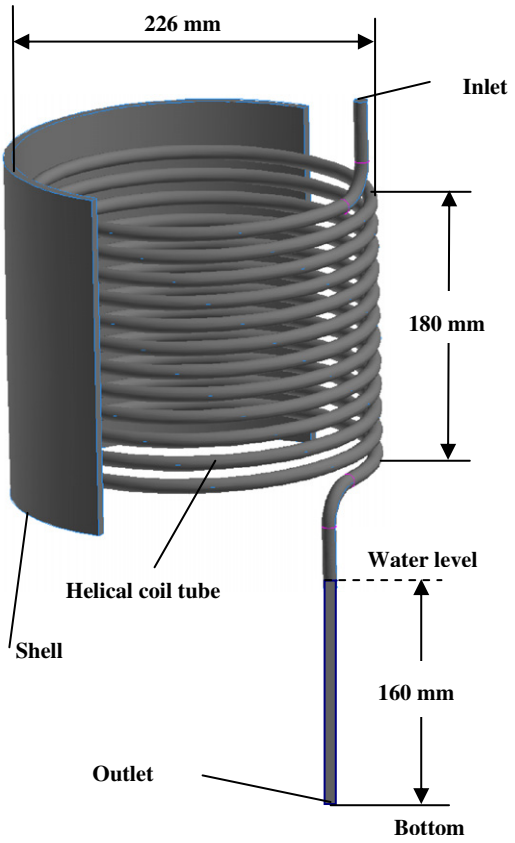

Fig. 3. Shell and helical coil tube condenser.

The experimental facility requires about 2–3 h to attain a steady-state condition after starting an experimental run. The steady-state condition was inferred when fluctuation of the measurement parameters was within their measurement accuracy for at least 20 min. All measurements were then averaged over 30–40-min intervals. Such a long interval is necessary because the condensed water flow rate is rather small. Throughout the day of the experiment, the pressure and temperature before the expansion valve were changed to vary the CO_2 quality at the condenser inlet. All other parameters were left unchanged.

3. Numerical model

Fig. 3 shows that numerical local heat transfer model with steam condensation and liquid CO_2 boiling was developed for the condenser with a shell and a helical coil tube of the new waste heat recovery system. In a coil tube with N turns, because one turn of the coil tube is located directly above another turn of the coil tube, the condensate falling behavior from one turn to the turn below can resemble that of N horizontal tubes placed one above the other. Because the coil inclination angle is approximately 1.2°, the coil tube might be regarded as a horizontal tube. In addition, because the ratio of the coil diameter (226 mm) to the tube outer diameter (9.53 mm) is approximately 24, the coil tube can be regarded as a straight tube. The steam condensation

heat transfer of the helical coil tube with N turns might be close to that in the horizontal N-tube bank.

For this study, a steam condensation heat transfer model on the helical coil tube was constructed based on the assumption that the heat transfer model obtained for the 14-tube bank is applicable to the present helical coil tube. This assumption was confirmed through comparison of numerical results calculated using the model with experimental data.

The modified Nusselt's correlation proposed by Kern [2] for a film condensation local heat transfer coefficient on a horizontal tube bank, h_{steam}, with an array of N horizontal tubes is given as

$$h_{steam} = 0.729N^{-1/6}\left[\frac{g\rho_l(\rho_L-\rho_V)h^*_{fg}\lambda_L^3}{\mu_L(T_{sat}-T_{wall})D}\right]^{1/4}. \quad (1)$$

This correlation well predicted experimental results for the number of the tube bank from 9 to 15 [14]. For that reason, this correlation is applied to the present numerical model.

The flow boiling heat transfer model proposed by Kattan [15] and recently updated by Thome and El Hajal for horizontal in-tube CO_2 evaporation [16] is given as

$$h_{tp} = \frac{R_{in}(2\pi-\theta_{dry})h_{wet}+R_{in}\theta_{dry}h_V}{2\pi R_{in}}. \quad (2)$$

A simplified two-phase flow structure is shown in Fig. 4. The heat transfer coefficient on the wetted tube surface, h_{wet}, is obtained as a combination of a nucleate boiling heat transfer coefficient, h_{nb}, and a convective boiling heat transfer coefficient, h_{cb}, as

$$h_{wet} = (h_{nb}^3 + h_{cb}^3)^{1/3}, \quad (3)$$

where h_{nb} is calculated according to the following Cooper correlation [17]:

$$h_{nb} = 55Pr^{0.12}(-\log_{10}Pr)^{-0.55}M^{-0.55}q^{0.67}, \quad (4)$$

while h_{cb} is given as

$$h_{cb} = 0.0133Re_L^{0.69}Pr_L^{0.4}\frac{\lambda_L}{\delta}. \quad (5)$$

Fig. 4 shows that the thickness of annular liquid film, δ, is calculable for the truncated annular ring using the same area occupied by the liquid. The vapor-phase heat transfer coefficient, h_V, calculated with the Dittus–Boelter turbulent flow heat transfer correlation [18], and assuming tubular flow over the tube dry surface, is derived as

$$h_V = 0.023\left(\frac{GxD}{\varepsilon\mu_V}\right)^{0.8}\left(\frac{C_{pV}\mu_V}{\lambda_V}\right)^{0.4}\frac{\lambda_V}{D}. \quad (6)$$

For simplification, the dryout angle was assumed to be zero for intermittent and annular flow; it varied linearly to 2π with vapor quality for stratified-wavy and mist flows. The flow pattern map for a high mass velocity of carbon dioxide ($\approx$650 kg/m^2 s) was taken from Ref. [9].

The heat balance in each elementary segment of condenser tube might be written in the following form

$$\begin{cases} h_{steam}(T_{steam}-T_{wall,out})2\pi R_{out}dL = dQ, \\ \lambda_{wall}\frac{(T_{wall,out}-T_{wall,in})}{\ln(R_{out}/R_{in})}2\pi dL = dQ, \\ h_{tp}(T_{wall,in}-T_{CO_2})2\pi R_{in}dL = dQ. \end{cases} \quad (7)$$

The nonlinear equation set of Eqs. (1)–(7) was solved interactively assuming that CO_2 pressure changes linearly along the length of the condenser tube. The heat transfer characteristics of the condenser were calculated along with the condenser tube length: heat flux, CO_2 boiling heat transfer coefficient, condensing heat transfer coefficient, CO_2 quality, heat load, etc. The numerical overall heat transfer coefficient, U_{calc}, obtained from the following equation Eq. (8) was compared to that of experimental data.

$$U_{calc} = \frac{Q_{calc}}{A_{out}(T^{sat}_{H_2O}-T^{sat}_{CO_2})}. \quad (8)$$

The heat load, Q_{calc}, was calculated by integrating the heat flux, $(dQ/2\pi R_{out}dL)$, along the condenser tube length.

Thermophysical properties of CO_2 were calculated using the NIST Standard Reference Database 12 [19]. To calculate the CO_2 properties for local HTC estimation the CO_2 pressure is assumed to be a linear function along the condenser length. It means that the inlet and outlet pressure are taken from the experimental data. This method allows to avoid mistakes in the CO_2 properties calculation caused by any pressure drop correlations for CO_2. The pressure drop of two-phase CO_2 was also estimated using an analytical model described in Ref. [20]. Steam properties were referenced from the PROPATH database [21].

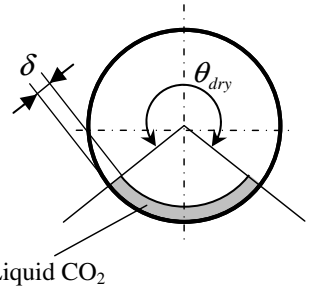

Fig. 4. Simplified two-phase flow structure in a horizontal tube.

4. Results and discussion

The steam condensing heat transfer rate, Q_{H_2O}, was evaluated from the enthalpy $i^4_{H_2O}$ and $i^5_{H_2O}$, which were evaluated from the temperature measurements at positions 4 and 5 in Fig. 2, and water flow rate, W_{H_2O}, as

$$Q_{H_2O} = W_{H_2O}(i^5_{H_2O}-i^4_{H_2O}). \quad (9)$$

The CO_2 side heat transfer rate, Q_{CO_2}, was evaluated similarly as

$$Q_{CO_2} = W_{CO_2}(i^1_{CO_2}-i^3_{CO_2}). \quad (10)$$

The experimental overall heat transfer coefficient of the condenser, U_{exp}, can be calculated using Eq. (11):

$$U_{exp} = \frac{(Q_{H_2O} + Q_{CO_2})/2}{A_{out}(T^{sat}_{H_2O} - T^{sat}_{CO_2})}, \quad (11)$$

where the saturation temperature of the CO_2 side, $T^{sat}_{CO_2}$, is calculated for the average CO_2 pressure and A_{out} is the heat transfer area of the condenser tube's outer surface. The heat loss from the condenser vessel surface to the ambient is judged to be very small because the difference between Q_{H_2O} and Q_{CO_2} is less than 1%. Therefore, the average value of Q_{H_2O} and Q_{CO_2} was used as the heat load. In all cases, the CO_2 superheating at the condenser outlet was maintained at 5 °C.

The condenser heat load decreases with the CO_2 inlet quality, as shown in Fig. 5. During the experiment, the CO_2 inlet quality is controlled by the CO_2 temperature before the expansion valve (position 1 in Fig. 2). The increase of the CO_2 temperature decreases the CO_2 inlet quality, which is calculated assuming adiabatic expansion in the expansion valve.

The overall heat transfer coefficient given in Fig. 6 decreases rapidly with the CO_2 inlet quality. The maximal value of overall heat transfer coefficient reaches approximately 4.4 kW/m^2 K, which is two times higher than the overall heat transfer coefficient of a conventional water-cooled condenser.

The numerical local heat transfer coefficients under the typical experimental conditions, given in Table 2, are shown in Fig. 7. The numerical and experimental overall heat transfer coefficients were evaluated from Eqs. (8) and (11). Fig. 8 shows that the numerical results of the overall heat transfer coefficient agree well with the experimental ones within a deviation range of about ±5%. Numerical estimations showed that among all the experimental conditions the CO_2 boiling local heat transfer coefficient reaches its maximum value of 26 kW/m^2 K at the inlet of the CO_2 side. This value is almost one order higher than that in a conventional water-cooled condenser. The

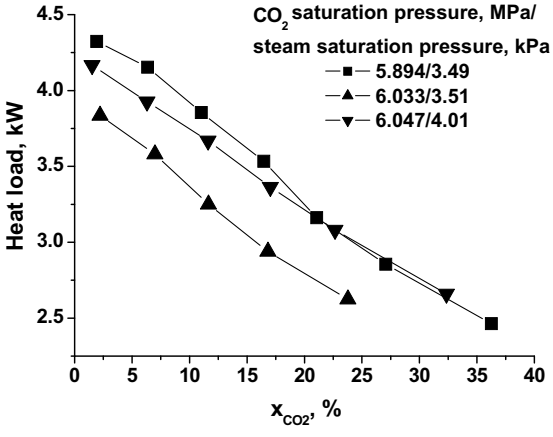

Fig. 5. Experimental condenser heat load as a function of CO_2 inlet quality.

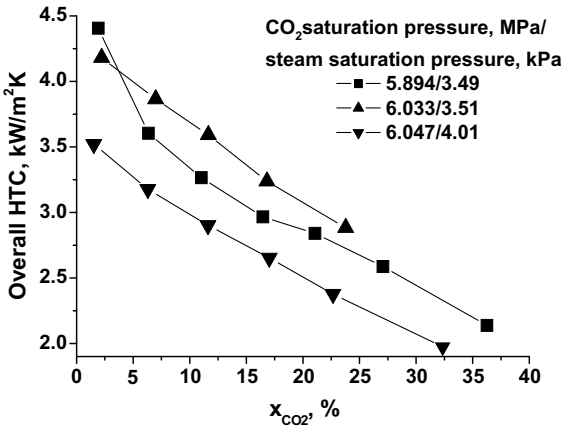

Fig. 6. Experimental overall heat transfer coefficient as a function of CO_2 inlet quality.

Table 2
Typical experimental condition

$P^{in}_{CO_2}$ (MPa)	$P^{out}_{CO_2}$ (MPa)	W_{CO_2} (kg/h)	$x^{in}_{CO_2}$	P_{steam} (kPa)
5.92	5.75	95.5	0.001	3.31

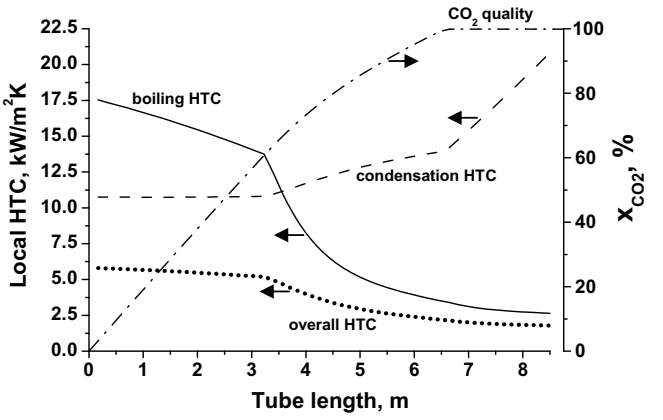

Fig. 7. Numerical local heat transfer coefficients along the condenser tube length.

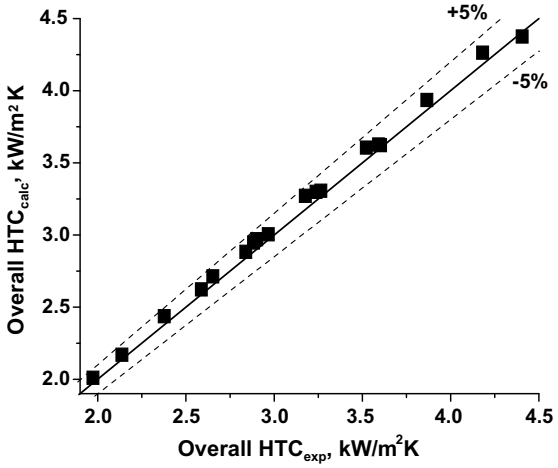

Fig. 8. Numerical vs. experimental overall heat transfer coefficient.

Table 3
Heat transfer performance of different types of condensers

Condenser	Conventional	New
Coolant	Seawater	Liquid CO_2
Cold side h, kW/m^2 K	3	8
Steam side h, kW/m^2 K	12	12
Overall HTC, kW/m^2 K	2.4	4.8
Relative heat transfer area	2	1

corresponding maximal heat flux, as estimated numerically, is as high as 59 kW/m^2. Overall heat transfer coefficients were also evaluated for a traditional steam condenser of the same geometry cooled by water, applying the Gnielinski equation [22] to calculate the water-side local heat transfer coefficient. Table 3 shows that the required heat transfer area is twice that of condenser cooled by liquid CO_2 boiling. The overall heat transfer coefficient is governed mainly by the CO_2 boiling heat transfer coefficient because its value is less than the steam condensing heat transfer coefficient. Consequently, the design process of CO_2-cooled condenser will be affected mainly by the accuracy of CO_2 boiling heat transfer estimation. However, it is difficult to estimate from experimental results how well the empirical correlations for CO_2 boiling heat transfer apply to the entire range of CO_2 quality.

At the exit of condenser, the CO_2 gas was superheated by 5 °C to ensure that no liquid CO_2 entered the CO_2 compressor. For that reason, the last few meters of the condenser tube are cooled by gaseous CO_2. The local heat transfer coefficient of gaseous CO_2 is smaller than that of boiling liquid CO_2. Therefore, the required heat transfer area is only different by twice its area, despite the fact that the maximal boiling local heat transfer coefficient is almost one order higher than that in the conventional condenser cooled by water. If an internal suction-to-supercritical line heat exchanger (Fig. 2, the inlet of hot water supplier-outlet of condenser) is provided, the CO_2 superheating might be set to zero. In that case, no 'gaseous CO_2-steam' heat exchange is involved and the condenser requirements for an adequate heat transfer area might be even further reduced.

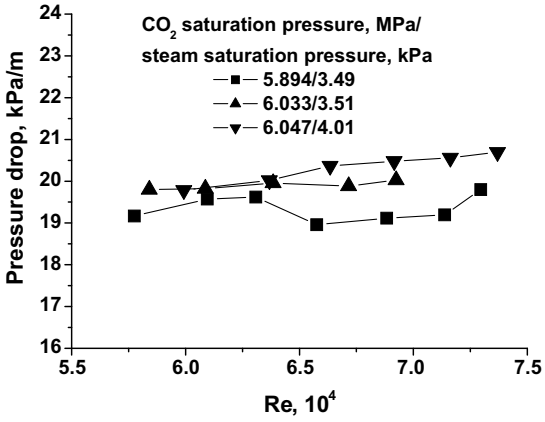

Fig. 9. Experimental pressure drop vs. CO_2 side Reynolds number.

The pressure drop is plotted against the Reynolds number in Fig. 9. Its value is in a range of 19–20.5 kPa/m. The pressure drop increases slightly with the Reynolds number, although it is almost independent of the CO_2 inlet quality. The pressure drop calculated using an analytical model described in Ref. [19] appears to be 3.2–3.5 times less than the experimental pressure drop. No explanations exist for that fact.

5. Conclusions

A steam condensing-liquid CO_2 boiling heat transfer model, which was developed for a steam condenser of a new waste heat recovery system, reproduces the overall heat transfer coefficients obtained experimentally within a range of ±5%. Numerical estimations showed that the boiling local heat transfer coefficient reaches its maximal value of 26 kW/m^2 K at the inlet of CO_2 side, which is almost one order higher than the local heat transfer coefficient of the conventional water-cooled condenser. The corresponding maximal heat flux is as high as 59 kW/m^2. The required heat transfer area of the condenser cooled by liquid CO_2 is half that of a traditional condenser.

Appendix A
Experimental raw data

Nos.	Parameter								
	CO_2 side						Steam side		
	P_1 (MPa)	T_1 (°C)	P_2 (MPa)	T_2 (°C)	W_1 (kg/h)	ΔP_{2-3} (kPa)	P_5 (kPa)	T_5 (°C)	W_4 (kg/h)
1	10.52	27.6	6.06	25.9	90.8	180	3.71	38.0	5.99
2	10.51	29.5	6.08	27.5	89.8	183	4.01	39.1	5.96
3	10.53	31.5	6.08	27.7	88.0	182	4.02	38.5	5.54
4	9.88	27.2	5.92	25.6	95.5	168	3.31	35.9	6.37
5	9.89	29.1	5.90	26.2	93.9	163	3.51	36.5	6.22
6	9.90	31.1	5.89	26.2	90.7	162	3.52	36.7	5.73
7	9.90	33.2	5.86	26.1	87.2	161	3.52	36.5	5.31

Appendix A (*continued*)

Nos.	Parameter								
	CO_2 side						Steam side		
	P_1 (MPa)	T_1 (°C)	P_2 (MPa)	T_2 (°C)	W_1 (kg/h)	ΔP_{2-3} (kPa)	P_5 (kPa)	T_5 (°C)	W_4 (kg/h)
8	9.92	35.1	5.90	26.0	82.9	167	3.52	36.4	4.75
9	9.93	37.2	5.91	26.1	80.0	166	3.52	36.5	4.29
10	9.95	39.8	5.88	26.1	76.2	163	3.52	36.5	3.70
11	9.86	28.4	6.05	25.9	88.3	170	3.52	36.3	5.63
12	9.87	30.4	6.04	25.9	85.8	169	3.52	36.4	5.32
13	9.90	32.3	6.05	25.9	81.4	170	3.52	36.4	4.94
14	9.92	34.3	6.05	26.0	77.6	169	3.52	36.5	4.40
15	9.94	36.6	6.05	26.0	74.5	168	3.52	36.5	3.92
16	9.86	28.3	6.08	27.6	93.4	176	3.96	38.2	6.25
17	9.85	30.3	6.07	27.9	91.0	175	4.02	38.2	5.84
18	9.86	32.2	6.04	27.9	88.4	174	4.02	38.3	5.53
19	9.89	34.2	6.03	27.9	85.0	173	4.02	38.2	5.07
20	9.91	36.1	6.01	28.0	81.8	170	4.02	38.2	4.61
21	9.94	38.9	5.98	28.1	77.6	168	4.02	38.3	4.02

The notations accord with those of Fig. 2.

References

[1] Y. Kato, T. Nitawaki, Waste heat recovery system for combined cycle power plants, 6th Gustav Lorentzen Natural Working Fluid Conf., Glasgow, UK, 2004, paper 5b.

[2] D.Q. Kern, Mathematical development of loading in horizontal condensers, J. Am. Inst. Chem. Eng. 4 (2) (1958) 157–160.

[3] Y. Hwang, B.H. Kim, R. Radermacher, Boiling heat transfer correlation for carbon dioxide, International Conference on Heat Transfer issues in Natural Refrigerants, University of Maryland, 1997, pp. 81–95.

[4] D.L. Bennett, J.C. Chen, Forced convective boiling in vertical tubes for saturated pure components and binary mixtures, AIChE J. 26 (1980) 454–461.

[5] A. Bredesen, A. Hafner, J. Pettersen, P. Neksa, K. Aflekt, Heat transfer and pressure drop for in-tube evaporation of CO_2, International Conference on Heat Transfer issues in Natural Refrigerants, University of Maryland, 1997.

[6] H.J. Hogaard Knudsen, P.H. Jensen, Heat transfer coefficient for boiling carbon dioxide. Workshop Proceedings – CO_2 Technology in Refrigeration, Heat Pump and Air Conditioning Systems, Trondheim, Norway, 1997, pp. 319–328.

[7] M.M. Shah, A general correlation for heat transfer during film condensation inside of pipes, Int. J. Heat Mass Transfer 22 (1979) 547–556.

[8] S.H. Yoon, E.S. Cho, Y.W. Hwang, M.S. Kim, K. Min, Y. Kim, Characteristics of evaporative heat transfer and pressure drop of carbon dioxide and correlation development, Int. J. Refrig. 27 (2004) 111–119.

[9] J.R. Thome, J. El Hajal, Flow boiling heat transfer to carbon dioxide: general prediction method, Int. J. Refrig. 27 (2004) 294–301.

[10] Z. Liu, R.H.S. Winterton, A general correlation for saturated and subcooled flow boiling in tubes and annuli based on a nucleate pool boiling equation, Int. J. Heat Mass Transfer 34 (1991) 2759–2766.

[11] R. Yun, Y. Kim, M.S. Kim, Y. Choi, Boiling heat transfer and dryout phenomenon of CO_2 in a horizontal smooth tube, Int. J. Heat Mass Transfer 46 (2003) 2353–2361.

[12] S. Koyama, S. Lee, D. Ito, K. Kuwahara, H. Ogawa, Experimental study on flow boiling of pure CO_2 and CO_2-oil mixtures inside horizontal smooth and micro-fin copper tubes, in: Proceedings of 6th IIR-Gustav Lorentzen Conference, Glasgow, UK, 2004, paper 1340.

[13] J.R. Thome, G. Ribatski, "State-of-the-art of two-phase flow and flow boiling heat transfer and pressure drop of CO_2 in macro- and micro-channels", review, Int. J. Refrig. 28 (8) (2005) 1149–1168.

[14] P.J. Marto, An evaluation of film condensation on horizontal integral-fin tubes, Trans. ASME, J. Heat Transfer 110 (1988) 1287–1305.

[15] N. Kattan, J.R. Thome, D. Favrat, Flow boiling in horizontal tubes. Part 3: development of a new heat transfer model based on flow patterns, J. Heat Transfer 120 (1998) 156–165.

[16] J.R. Thome, Update on advances in flow pattern based two-phase heat transfer models, Exp Therm Fluid Sci. 29 (3) (2005) 341–349.

[17] M.G. Cooper, Heat flow rates in saturated nucleate pool boiling – a wide-ranging examination of reduced properties, Adv. Heat Transfer 16 (2) (1984) 157–239.

[18] F.W. Dittus, L.M.K. Boelter, Heat transfer in automobile radiators of the tubular type, Publications in Engineering. 2. University of California, Berkeley, 1930, pp. 443–461.

[19] E.W. Lemmon, A.P. Peskin, M.O. McLinden, D.G. Friend, NIST standard reference database 12: NIST thermodynamic and transport properties of pure fluids, Version 5.0, National Institute of Standards and Technology, Standard reference data program, 2000.

[20] S.J. Smith, L. Shao, S.B. Riffat, Pressure drop of HFC refrigerants inside evaporator and condenser coils as determined by CFD, Appl. Energy 70 (2001) 169–178.

[21] PROPATH Ver. 10.2, Kyushu University, Fukuoka, Japan, 2004.

[22] V. Gnielinski, New equations for heat and mass transfer in turbulent pipe and channel flow, Int. Chem. Eng. 16 (1976) 359.